Published in final edited form as:

Biochim Biophys Acta Mol Basis Dis. 2019 November 01; 1865(11): 165527. doi:10.1016/j.bbadis.2019.08.003.

Role of endothelin receptor type A on catecholamine regulation in the olfactory bulb of DOCA-Salt hypertensive rats: Hemodynamic implications

María J. Guil[1,2], **Mercedes I. Schöller**[1,2], **Luis R. Cassinotti**[1,2,*], **Vinicia C. Biancardi**[3,*], **Soledad Pitra**[3], **Liliana G. Bianciotti**[4,5], **Javier E. Stern**[3,*], **Marcelo S. Vatta**[1,2]

[1]Universidad de Buenos Aires, Facultad de Farmacia y Bioquímica, Cátedra de Fisiología, Buenos Aires, Argentina

[2]CONICET-Universidad de Buenos Aires, Instituto de Química y Metabolismo del Fármaco (IQUIMEFA), Buenos Aires, Argentina.

[3]Department of Physiology, Augusta University, Augusta, GA, USA.

[4]Universidad de Buenos Aires, Facultad de Farmacia y Bioquímica, Cátedra de Fisiopatología, Buenos Aires, Argentina

[5]CONICET-Universidad de Buenos Aires, Instituto de Inmunología, Genética y Metabolismo (INIGEM), Buenos Aires, Argentina.

Abstract

Increasing evidence shows that the olfactory bulb is involved in blood pressure regulation in health and disease. Enhanced noradrenergic transmission in the olfactory bulb was reported in hypertension. Given that endothelins modulate catecholamines and are involved in the pathogenesis of hypertension, in the present study we sought to establish the role of the endothelin receptor type A on tyrosine hydroxylase, the rate limiting enzyme in catecholamine biosynthesis, in the olfactory bulb of DOCA-salt hypertensive rats.

Sprague-Dawley male rats, randomly divided into Control and DOCA-Salt hypertensive groups, were used to assess endothelin receptors by western blot and confocal microscopy, and their co-localization with tyrosine hydroxylase in the olfactory bulb. Blood pressure and heart rate as well as tyrosine hydroxylase expression and activity were assessed following BQ610 (ET_A antagonist)

Corresponding author: Marcelo S. Vatta PhD, Cátedra de Fisiología, Facultad de Farmacia y Bioquímica, Universidad de Buenos Aires, Junín 956 – Piso 7, 1113AAD Buenos Aires, Argentina. Tel.: +54-11-5287-4709. Fax: +54-11-4508-3645. mvatta@ffyb.uba.ar.

Author Contributions

MJG and MSV conceived and designed the experiments; MJG performed the experiments; MIS, LRC, VCB and SP collaborated in the experiments; MJG, JES and MSV analyzed the data; MJG, LGB, JES and MSV wrote the paper.

*Current address:

LRC: Kresge Hearing Research Institute, University of Michigan Medical School, Ann Arbor, MI, USA

VCB: Department of Anatomy, Physiology and Pharmacology, College of Veterinary Medicine, Auburn University, Auburn, AL, USA

JES: Neuroscience Institute, Center for Neuroinflammation and Cardiometabolic Diseases, Georgia State University, Atlanta, GA, USA

applied to the brain. DOCA-Salt hypertensive rats showed enhanced ET_A and decreased ET_B expression. ET_A co-localized with tyrosine hydroxylase positive neurons. Acute ET_A blockade reduced blood pressure and heart rate and decreased the expression of total tyrosine hydroxylase and its phosphorylated forms. Furthermore, it also diminished mRNA tyrosine hydroxylase expression and accelerated the enzyme degradation through the proteasome pathway as shown by pretreatment with MG132, (20s proteasome inhibitor) intracerebroventricularly applied.

Present findings support that the brain endothelinergic system plays a major role through ET_A activation in the increase of catecholaminergic activity in the olfactory bulb of DOCA-Salt hypertensive rats. They provide rationale evidence that this telencephalic structure contributes in a direct or indirect way to the hemodynamic regulation in salt dependent hypertension.

Keywords

DOCA-Salt rats; endothelin; endothelin receptors; experimental hypertension; olfactory bulb; tyrosine hydroxylase

1. Introduction

The central nervous system (CNS) has a major role in the short and long term regulation of cardiovascular activity in health and disease [1]. The solitarii tract nucleus, brain stem, the hypothalamus, the rostral ventrolateral medulla, and the locus coeruleus are well established brain structures intimately involved in cardiovascular regulation. However, despite strong evidences in the literature, the contribution of other regions like the olfactory bulb (OB) has been overlooked [2–4]. This telencephalic region is divided into the main and the accessory OB and connects with areas involved in blood pressure regulation and cardiac function, like the amygdala, piriform cortex, septum, hypothalamus, locus coeruleus and grey periaqueductal area [5–7].

The olfactory system is related to behavioral and stress responses to odor conditioning. A recent study showed the effects of predator odor fear stimuli in the modulation of autonomic activity, endocrine secretion and behavior, stressing the relevance of hypothalamic structures and showing that the signaling pathways responsible for such changes involved the OB [8]. Various studies support a clear link between the sympathetic nervous system and the OB [9]. Early works showed that olfactory stimulation correlates with respiratory and blood pressure changes in dogs [10]. Furthermore, blood pressure, breathing and sympathetic discharge increase when conscious rats are exposed to smoke whereas the opposite occurs when animals are exposed to lavender oils [9,11,12]. Changes in rat vascular and cardiac physiology correlate with norepinephrine (NE) levels in the OB, suggesting that olfactory stimulation enhances sympathetic activity and blood pressure through a multisynaptic pathway connecting the OB with brain autonomic centers [6,13]. Recent studies from our laboratory show that catecholaminergic transmission in the OB is enhanced DOCA-Salt hypertensive rats [14]. Despite growing evidence, the role of the OB in the regulation of cardiovascular function has not been fully established [15,16].

The removal of the OB significantly increases NE content and monoamine oxidase activity in the brainstem [17]. Partial or total OB removal results in behavioral, endocrine, immune, and cardiovascular changes as a consequence of modifications in brain neurotransmitters like NE, serotonin, glutamate and GABA [6,18–20]. It was also reported that a normal sympathoexcitatory response to physiological stimuli like the baroreflex is dependent on the integrity of the OBs [4].

The OB expresses all components of the endothelinergic system including the endothelin (ET) converting enzyme and both ET receptors (ET_A and ET_B). The ET_A receptor is mainly located in the glomerular layer (GL) where the sensory information is processed [21,22]. Previous *ex vivo* studies from our laboratory show that ETs applied to the brain increase tyrosine hydroxylase (TH, EC 1.14.16.2) expression and activity in the OB of normotensive rats [23,24]. Although ET_A and TH are expressed in the OB, their possible co-localization and the ETs-catecholamine interaction have not been yet investigated.

Hypertension is a multifactorial complex disease where genetic, dietary and environmental factors combine resulting in chronic blood pressure elevation. The role of brain catecholamines, particularly NE, in the pathogenesis of hypertension in animals and humans has been well documented. Lesions in central catecholaminergic areas attenuate hypertension in DOCA-Salt hypertensive rats and spontaneously hypertensive rats (SHR) [25,26]. Also, blood pressure elevation resulting from increased salt intake correlates with changes in brain catecholamines. Numerous studies support that the overactivity of the sympathetic nervous system and the impairment of the renin-angiotensin system are crucial events in the development of hypertension [27–29]. The DOCA-salt hypertensive rat is a neurogenic hypertensive animal model characterized by hypervolemia and hyperaldosteronism, as well as enhanced salt intake, sympathetic tone and plasma ET-1 [26, 30]. It also shows brain ET-1 mRNA overexpression and blood pressure reduction following an ET_A antagonist applied to the periaqueductal grey area [31,32]. Noradrenergic activity is enhanced in the posterior hypothalamus of DOCA-Salt rats exposed to ET-1 and ET-3, which may be partially responsible for the overactivity of the sympathetic nervous system observed in this animal model [33]. In a recent study, we showed that chronic ET_A blockade reduces blood pressure and prevents catecholaminergic overactivity in the OB of DOCA-salt hypertensive rats [34]. However, the interaction between ETs and catecholaminergic neurons in acute blood pressure regulation has not been assessed.

Given that noradrenergic transmission and the ET system are enhanced in the OB of DOCA-salt hypertensive rats, we sought to establish the role of ET_A receptors on TH (the rate limiting enzyme and master regulator of catecholamine synthesis) and its impact on hemodynamic parameters in an attempt to advance in the knowledge of the role of the OB in salt dependent hypertension.

2. Methods

2.1. Chemicals

The following drugs and reagents were used: DOCA (MP Biomedicals, LLC OH, USA); BQ610 (American Peptide Company California, USA); MG132, N-succinyl-Leu-Leu-Val-

Tyr 7-amido-4-methylcoumarin, catalase, tetrahydrobiopterin, l-tyrosine, protease inhibitor cocktail, anti-actin polyclonal antibody, anti-TH monoclonal antibody (Sigma-Aldrich, MO, USA); ^{3}H L-tyrosine (Perkin Elmer, MA, USA); PVDF membrane (GE Healthcare, Amersham Biosciences UK); anti-TH-PSer40 polyclonal antibody, anti-TH-PSer31 polyclonal antibody, anti-TH-PSer19 polyclonal antibody, and HRP anti-mouse conjugated antibody (EMD Millipore, CA, USA); anti-ubiquitin polyclonal antibody, A/G protein, and HRP conjugated anti-rabbit antibody (Santa Cruz, TX, USA); anti-ET_A polyclonal antibody and anti-ET_B polyclonal antibody (Alomone Jerusalem, Israel); anti-Rabbit-Alexa488 antibody, and anti-Mouse-Alexa594 antibody (Jackson, PA, USA), quimioluminicent reaction kit (Kalium Technologies, Buenos Aires, Argentina), Tri Reagent (Molecular Research, OH, USA), RNAsin (Genbiotech, Buenos Aires, Argentina); DNAsa kit, RLVM kit, and Go-Taq (Promega, WI, USA), Oligo dT (Genbiotech, Buenos Aires, ARG), Primers (IDT, Buenos Aires, Argentina), Eva Green 20X (Biotium, CA, USA), dNTPs, and Taq Pegasus (Productos Bio-lógicos, Buenos Aires, Argentina). Other reagents were of analytical or molecular biology quality and obtained from standard sources.

2.2. Animals

Male Sprague-Dawley rats weighting between 100 and 130 gr. (from the School of Pharmacy and Biochemistry, University of Buenos Aires) were used in the experiments. Animals were housed four per cage under a 12 hs light/dark cycle, maintained with controlled temperature (22 ± 2 °C) and humidity (45 – 55%), and fed with standard commercial chow diet (Gepsa Feeds, Grupo Pilar, Pilar, Córdoba, Argentina) and water *ad libitum*. All experiments were performed following the principles of the *Guide for Care and Use of Laboratory Animals* and the *International Guiding for Biomedical Research Involving Animals*. The experimental protocols were approved by the Institutional Animal Care and Use Committee of the School of Pharmacy and Biochemistry, University of Buenos Aires (N° 031013-5; EXP-FYB N° 56106/13). All efforts were made to minimize the number and suffering of used rats. DOCA-salt hypertension was induced by subcutaneous injections of DOCA (15 mg/kg twice a week) and by the administration of 1% NaCl in the drinking water for five weeks. At week five animals were anesthetized and brains prepared for fluorescence microscopy studies as detailed below. Another set of animals were anesthetized at week 4 in order to place a guide cannula in the brain lateral ventricle for the administration of drugs as described below.

2.3. Experimental protocols

2.3.1 Expression of ET receptors in the OB of normotensive and DOCA-salt hypertensive rats.—

At the end of the fifth week of treatment, Control and DOCA-Salt rats were euthanized by decapitation. OB were rapidly dissected and collected in cold homogenization buffer for western blot assay.

2.3.2 Expression of ET receptors and TH in the OB of normotensive and DOCA-Salt hypertensive rats by fluorescent immunohistochemistry—

At week five, rats were anesthetized with urethane (1 g/kg, ip) and transcardially perfused with 0.01 M phosphate-buffered saline (PBS) followed by 4% paraformaldehyde. Brains were post-fixed in 4% paraformaldehyde for 3 h at 4°C. Fixed brains were cryoprotected at 4°C with

0.01 M PBS containing 30% sucrose for 48 h. Sections (50 μm) were then cut with a cryostat (Leica CM 3050 S) and preserved for further assays. Normotensive and hypertensive brains were processed by pairs separately. The procedures were followed in a blinded way to avoid bias. Random numbers were assigned to tissues and a different operator formed the normotensive and hypertensive pairs. Incubations were made by the floating technique at room temperature with a rocking agitator.

OB slices were exposed to 0.01 M PBS containing 0.3% Triton X-100, 0.04% NaN3 and 10% normal horse serum for 1 h. Sections were then incubated overnight with the following primary antibodies: anti-ET_A rabbit (1:500) and anti-TH mouse (1:10.000); or anti-ET_B rabbit (1:500) and anti-TH mouse (1:10.000). Incubation with primary antibodies were followed by washes with PBS solution and exposed to secondary antibodies (anti-rabbit-Alexa 488 and anti-mouse-Alexa 594, 1:250) for 4 h in the dark. Antibodies were diluted in PBS containing 0.3% Triton X-100 and 0.04% NaN3. Histological sections were examined with a Zeiss LSM 510 confocal microscope system (Carl Zeiss, Oberkochen, Germany). The argon-krypton laser was used to excite the Alexa-488 (488 nm), He-Ne (561 nm) for the Alexa-594 fluorophores, and the diode (405 nm) for DAPI excitation. Fluorescent signal cross-talk among channels was avoided by setting image-acquisition parameters with individually labelled sections, ensuring a lack of “bleed through” to other channels. Images were taken with a 25X- LC Plan-Neofluar (oil)- NA 0.8 objective. Each picture was taken with a 1.5 um step in z axis, for a total of 10 um (8 images total) and a 1X optic zoom. From the selected area, a subregion containing the border of the glomerular lumen expressing TH positive body neurons was chosen for greater magnification (image with a 2.8X optic zoom) in order to further investigate the distribution of the TH and ET receptors.

Quantitative approaches: The images from each channel were analyzed with the ImageJ software and with a specific colocalization plugin. Initially, images were z projected with a maximum intensity and the type of the image was changed to 8 bits. Colors were then split. Threshold, quantification and colocalization were assessed in the ET_A, ET_B and TH images as explained below.

Threshold determination: In the images of ET_A, ET_B and TH, background intensity was assessed from areas with no positive stain. To objectively define a threshold value for each color and image, 6 areas with no positive immunostaining were depicted and saved using the ROI tool. At the same time, a visual value for threshold was defined according to the investigator criteria. A factor was then calculated relating those two thresholds. After performing this measurement in all images, the factor mentioned was averaged considering the frequency of appearance for each value. The number thusly obtained was used as a weighting factor to objectively measure background in the images

Area determination: The glomerular lumen (GLu) and the periglomerular area (PG) were depicted using the DAPI channel and saved with the ROI manager tool of the software. These sections were later reproduced in the images of ET_A and TH, or ET_B and TH, from the same set.

Quantification: Measures were made for each channel in the different glomerulus and periglomerular areas (saved as ROI), limited to the threshold value previously calculated (measurement on the 6 immuno-negative areas previously depicted and saved, multiplied by the weighting factor). Fluorescence intensity and positive immunoreactive area of ET_A, ET_B and TH were thusly calculated for both, normotensive and hypertensive rats. Immunofluorescence intensity (au) and area percentage of positive signal was plotted into graph bars for analysis and comparison.

Colocalization: The co-localization of TH with ET receptors was measured in the stack of confocal images z projected with maximum intensity from the different fluorophores. A co-localization plugin was used. Thresholds previously calculated for each channel during the quantification and ROIs depicted were used in this determination. Briefly, with the two images to analyze opened, after setting in the co-localization dialog which image was the red fluorophore and which the green (with the corresponding threshold for each color), two new images were created. One with the merged images and the co-localized pixels painted in white, and another image (8 bits plots) with only the pixels co-localized plotted. The later was the one used to quantify the area immune-positive for the co-localization. The periglomerular and glomerular areas were defined using the same ROIs (saved from the individual quantifications) in the corresponding images. Area percentage of co-localized signal was plotted into graph bars for analysis and comparison.

2.3.3 Effect of central ET_A blockade on hemodynamic parameters and TH in the OB of normotensive and DOCA-Salt hypertensive rats.—

At the end of week four, Control normotensive and DOCA-salt hypertensive rats were anesthetized with ketamine/xylazine (50/10 mg/Kg, IP) and a guide cannula was placed in the cerebral lateral ventricle. Briefly, animals under anesthesia were mounted in a stereotaxic apparatus, and a small hole was drilled through the skull. An intracranial cannula (21-gauge stainless steel, 1.5 cm in length) was placed into the left lateral ventricle by using appropriate stereotaxic coordinates (1.3 mm posterior to the bregma, 2.0 mm lateral to the midline, and 4.0 mm ventral to the skull surface). The cannula was secured by screws inserted into the surface of the bone using cyanoacrylate. Rats were placed in individual cages with free access to food and water and allowed to recover from surgery. One week later the animals were anesthetized with urethane (1 g/Kg, IP) and the femoral artery cannulated for blood pressure recording (AD Instruments PowerLab, Pty Ltd, Sydney, Australia). Following stabilization, artificial cerebrospinal fluid (aCSF) (control) or 20 μM BQ610 (selective ET_A antagonist) were intracerebroventricularly (icv) applied (1 μl) and blood pressure and heart rate were recorded for 60 min. Animals were then euthanized, and OBs rapidly removed for TH activity and expression assays.

Recordings were carefully reviewed avoiding artifacts using the blood pressure module in the Lab chart software. Then data of systolic blood pressure (SBP), diastolic blood pressure (DBP), mean arterial pressure (MAP) and heart rate (HR) were extracted and further analyzed to compare the effect of treatments and time before drug delivery and every 10 minutes following drug injection.

2.3.4 Effect of central ET_A blockade on hemodynamic parameters and TH in OB of normotensive and DOCA-salt hypertensive rats: Participation of the ubiquitin-proteasome system—In another set of animals and following the experimental procedure previously detailed, the participation of the ubiquitin-proteasome system in TH catabolism was evaluated by the icv administration of 20 μM MG132 10 min before BQ610 administration. MG132 is a synthetic tripeptide that displays a high cell penetration and inhibits reversibly the proteasome 26S complex, mainly the chymotrypsin-like activity [35]. The following groups were studied: aCSF (Control), MG132, BQ610, MG132+BQ610, DOCA-Salt, DOCA-Salt+MG132, DOCA-Salt+BQ610 and DOCA-Salt +MG132+BQ610.

2.4. Assays

2.4.1 Tyrosine hydroxylase activity—TH activity was assessed in the OBs by a radioenzymatic assay as previously detailed [36]. Results are expressed as percentage of Control ± SEM [23, 34].

2.4.2 Expression of TH and ETRs—The expression of total TH and its phosphorylated forms as well as ETRs (ET_A and ET_B) were assessed in the OB by western blot. Briefly, samples were separated with a 10% acrylamide gel (under denaturing and reducing conditions) after boiling for 5 min at 100°C. Proteins were then transferred to PVDF membranes, blocked with 5% non-fat milk, incubated overnight with primary antibodies at 4°C followed by secondary antibody incubation for 1 h at room temperature. Bands were detected with a quimioluminiscent kit, analyzed by densitometry and normalized to β-actin probed to the same membrane following stripping. Antibodies, working dilution and incubation periods are detailed in Table II. Results are expressed as percentage of Control ± SEM [23,33].

2.4.3 TH and ET_B mRNA determination—TH and ET_B mRNA was determined in the OB by quantitative real time RT-PCR as previously detailed [23]. The following primers were used: TH: 5'-AGGGCTGCTGTCTTCCTAC-3' (forward) and 5'-GCTGTGTCTGGGTCAAAGG-3 ' (reverse); β-actin: 5'-TCTGTGTGGATTGGTGGCTCTA-3' (forward) and 5'-CTGCTTGCTGATCCACATCTG-3' (reverse). PCR consisted in an initial denaturalization of 5 min at 94°C; a cycling of: denaturalization at 94°C 15 sec, annealing at 54°C 30 sec and extension at 72°C 30 sec (35 times); and a melting step rising from 77°C to 95° increasing 0.3°C per sec. ET_B quantification was performed using the following primers: forward 5'-CAAAGACTGGTGGCTGTTCAGTT-3' and reverse 5'-TCAAGGCAATCTGCATACCACTT-3'. The PCR consisted in an initial denaturalization of 5 min at 94°C; a cycling of: denaturalization at 94°C 30 sec, annealing at 59.5°C 50 sec and extension at 72°C 45 sec (35 times); and a melting step rising from 70°C to 95° increasing 0.5°C per sec. Results are expressed as a percentage of Control ± SEM [23].

2.4.4 Proteasome activity—Proteasome activity was assessed as described elsewhere [35] with minor modifications. Each dissected OB was homogenized in lysis buffer (6mM HEPES, 0.3 mM EDTA, 0.6 mM DTT, 84 mM sucrose; pH 7.4) and centrifuged at 18,000 g

for 10 min at 4°C. To assess proteasome activity samples were mixed with the reaction buffer (50 mM Tris-HCl, pH 7.40, 40 mM KCl, 5 mM MgCl, 2 % glycerol, 0.5 mg/ml BSA), DMSO, 60 mM ATP and 100 μM N-succinil-Leu-Leu-Val-Tyr- 7 Amido-4-metilcumarin in DMSO. Non-specific degradation was determined by adding 10 nM MG132 instead of DMSO alone. For blank reactions samples were replaced by water. Activity was measured by fluorometric detection (excitation 380 nm; emission 460 nm) for 1 h with a 6 sec interval (FlexStation III, Molecular Devices, Sunnyvale, CA, USA). The slope of fluorescence vs. time during the linear phase in each sample was normalized to its unspecific proteasome activity and total protein content. Results are expressed as percentage of control or DOCA-Salt ± SEM.

2.4.5 Co-immunoprecipitation with ubiquitin—Each sample (250 μg protein) was incubated with anti-ubiquitin antibody at 4°C for 90 min followed by the addition of AG protein-agarose and further incubated for 3 h at 4°C under shaking. Samples were then centrifuged at 1,000 g for 5 min at 4°C, pellets rinsed in PBS and resuspended in Laemmli buffer, centrifuged at 1,000g for 5 min at 4°C and freezed. Co-immunoprecipitated samples were separated the following day in a discontinuous SDS-page running polyacrylamide gel at 100 v and transferred to PDVF membranes. Bands were visualized and analyzed as previously described by measuring signal intensity over 60 kDa (TH molecular weight). Results are expressed as percentage of Control ±SEM.

2.5. Statistical Analysis

Results are expressed as mean ± SEM. Normal distribution was checked with the Shapiro-Wilk normality test. The Student's t test was used to compare the expression of ET receptors by western blot and quantitative RT-PCR, with the Welch's correction when variances were different. Hemodynamic parameters were analyzed by a two ways ANOVA with repeated measures over time followed by the Bonferroni post-test. TH parameters were analyzed by one-way ANOVA followed by Bonferroni post-test. Proteasome activity was assessed by the Student's t test with Welch's correction. In all cases p values of 0.05 or less were considered statistically significant.

3. Results

3.1. ETRs expression and co-localization with TH in OB neurons.

The expression of ETRs in the OB assessed by western blot showed that in DOCA-salt hypertensive rats ET_A expression was significantly increased as compared with normotensive animals, whereas that of ET_B receptors was diminished (Figures 1a and 1b). The expression of ET_B receptors was also assessed by quantitative RT-PCR showing that ET_B mRNA expression was also reduced in DOCA-salt hypertensive rats (Figure 1c).

ET_A and TH positive neurons are highly expressed in the OB GL of normal rats [21, 37-39]. It was shown that TH positive neural cell bodies localize in the PG zone and project to the GLu [40]. Given that the GL contains glomerular structures, results were referred to the GLu or the PG area. DOCA-Salt hypertensive rats showed increased TH expression in the OB as compared to normotensive animals (Figure 2a). Strong staining was observed in the GLu

and the PG area, but although TH staining was higher in the PG area rather than in the GLu in both normotensive and hypertensive rats, it was more widely distributed in the GLu. In DOCA-Salt hypertensive rats, TH positive cell bodies were increased in the PG region (Figure 2). ET_A receptor staining in hypertensive animals was increased by 224.6%, in the GLu and diminished by 30.7% in the PG, though this reduction was not statistically significant (Figure 2). These findings correlate well with western blot results (Figure 1). The percentage of ET_A immunoreactive area was not affected by hypertension at the glomerular or extraglomerular level. ET_A receptor distribution in the OB followed the same pattern in both normotensive and hypertensive animals. The expression of ET_B receptor was also similar, but the percentage of the immunoreactive area in the GLu was significantly diminished in hypertensive rats (Figure 2). Not only the intensity but also the percentage of the immunoreactive area followed the same pattern in both, GLu and PG area in normotensive and hypertensive animals. Furthermore, in both groups, the PG area showed higher ET_B receptor expression.

In hypertensive rats, co-expression of ETRs and TH showed ten-fold increase in ET_A/TH co-localization in the GLu without changes in the PG area, though both signals were lower in the PG area vs GLu in DOCA-Salt rats (Figure 2b). Co-localization of ET_B receptor and TH was increased in the GLu of hypertensive rats (Figure 2b). Representative images are shown in Figure 2c.

3.2. Acute brain ET_A blockade diminished systolic blood pressure in DOCA-Salt hypertensive rats.

Systolic blood pressure was registered before acute ET_A blockade. DOCA-Salt rats showed a significant increase in systolic blood pressure (148.2 ± 4.2 mmHg) as compared to control animals (114.3 ± 6.0 mmHg) ($p< 0.001$). No changes were observed in body weight between the two groups (data not shown).

Blood pressure and heart rate were monitored for 60 min following ET_A receptor antagonist administration. Control animals showed no changes in the haemodynamic parameters assessed following BQ610 administration (Figures 3 a-d). However, in DOCA-salt rats, the increase in systolic blood pressure was reduced by ETA blockade. The significant fall in BSP was evident at 30 min following BQ610 injection and remained diminished until the end of the experiment (Figure 3a). DBP and MAP in hypertensive animals showed a reducing trend after ETA blockade although it was not statistically significant (Figures 3 b). HR showed changes neither in normotensive nor hypertensive animals following BQ610 administration (Figure 3d). Figure 3e shows representative traces of changes in blood pressure and HR following ET_A blockade.

3.3. Acute brain ET_A blockade decreased the activity and phosphorylation of TH in DOCA-Salt hypertensive rats

TH activity was enhanced in the OB of hypertensive animals as previously reported [14]. Blockade of ET_A induced no changes in TH activity in normotensive animals, but it reduced the enzyme activity to control values in DOCA-Salt hypertensive rats (Figure 4a). TH has four potential phosphorylation Ser-sites, three of which are intimately implicated in the

activity of the enzyme (Ser19, Ser31 and Ser 40). Consistent with previous studies, the expression of TH-PSer19, TH-PSer31 and TH-PSer40 were increased in the OB of DOCA-Salt rats [14]. Blockade of ET_A by BQ610, decreased the expression of the phosphorylated forms of the enzyme to control levels in hypertensive animals but induced no changes in normotensive rats (Figures 4c and 4d). Surprisingly, ET_A blockade also decreased total TH protein expression in hypertensive rats (Figure 4b and c). This unexpected finding suggests TH premature degradation given the short-time exposure to the ET_A antagonist.

3.4. Acute brain ET_A blockade decreased total TH mRNA expression in DOCA-Salt hypertensive rats

As previously reported, TH mRNA was enhanced in hypertensive rats [14], but ET_A blockade significantly decreased it (Figure 4b). Again, given the short-term exposure to the ET_A antagonist, this finding suggested premature TH degradation.

3.5. Inhibition of proteasome activity prevented ET_A blockade effects on hemodynamic parameters and TH activity and expression

We next evaluated whether the decrease in TH expression observed in hypertensive animals resulted from premature proteolysis. As the ubiquitin-proteasome pathway is the major route for TH degradation, following the same experimental protocol animals were pretreated with MG132 (20S proteasome inhibitor) [35,41]. Systolic blood pressure was assessed before the initiation of the study in all animals. DOCA-Salt rats showed elevated systolic blood pressure (146.9 ± 4.4 mmHg) as compared to control rats (116.1 ± 5.0 mmHg) ($p< 0.001$). Body weigh was not different between the two groups (data not shown).

In normotensive rats, central inhibition of the proteasome activity had no significant effect on SBP, DBP, MAP and HR (Figure 5 a-d). Nevertheless, in DOCA-Salt rats, it prevented the fall in systolic blood pressure induced by ETA blockade (Figure 5a). The decreasing trend in DBP and MAP observed after ETA blockade in hypertensive animals was inhibited by MG132. (Figures 5b-c). HR showed no changes in either group when proteasome activity was inbibited. Representative traces of changes in blood pressure and HR are shown in Figure 5e.

TH activity and expression were also assessed in the OB of animals pretreated with MG132 in the presence or absence of B1610. In control rats, proteasome inhibition increased TH activity but no changes were observed when ET_A receptors were also blocked (Figure 6a). MG132 treatment did not change TH activity in the OB of hypertensive rats but it prevented the decrease induced by ET_A blockade, (Figure 6a).

MG132 also prevented the decrease in total TH expression induced by BQ610 (Figures 6c and 6d). Proteasome inhibition increased TH-PSer 19 expression in normotensive rats, but BQ610 inhibited it (Figures 6c and 6d). However, in hypertensive rats, while MG132 did not affect TH-PSer19 expression it partially inhibited BQ610 response (Figures 6c and 6d). Proteasome inhibition did not cause changes in the expression of TH-PSer31 and TH-PSer40 in control animals, but in DOCA-Salt rats it increased TH-PSer31 and, although it did not modify TH-PSer40, it prevented the response of the ET_A receptor activation (Figures 6c and 6d). Proteasome inhibition also inhibited BQ610 effect on TH mRNA in both

normotensive and hypertensive rats (Figure 6b). Effective proteasome inhibition by MG132 in the OB was corroborated by a fluorescent substrate of the 20S subunit. Results showed that MG132 applied to the brain partially inhibited proteasome activity in the OB of normotensive and hypertensive animals (Figure 7).

3.6. ET_A blockade enhanced TH ubiquitination in the OB of DOCA-Salt hypertensive rats

Present findings suggested an imbalance between TH synthesis and degradation, so we evaluated whether the enzyme was metabolized through the ubiquitin-proteasome pathway. The ubiquitin-proteasome system, through a concerted action of enzymes, mark proteins for proteasome degradation by liking them to ubiquitin. Therefore, ubiquitin-tagged TH in the OB was assessed showing that in normotensive animals, it was not changed by MG132 or ET_A blockade. However, in hypertensive rats BQ610 enhanced TH ubiquitination in the OB, which was not prevented by MG132 (Figure 8).

4. Discussion

The present study advances in the knowledge of the mechanisms involved in DOCA-Salt hypertension, particularly the role of brain ETs and catecholamines in the OB. The major findings were that in DOCA-Salt hypertension: 1.- ET_A expression was augmented in the OB whereas that of ET_B was diminished; 2.- TH and ET receptors co-localized in the GLu of the OB; and 3.- Brain ET_A blockade reduced systolic blood pressure and heart rate as well as TH activity and expression. These findings support overactivity of the endothelinergic system in the OB of DOCA-Salt hypertensive rats that leads to enhanced TH activity and expression. In addition, they further suggest an interaction between central ETs and the cardiovascular system since changes in TH induced by ET_A activation in the OB were associated with hemodynamic variations, which may contribute to blood pressure elevation in salt-dependent hypertension.

In the OB, TH expresses in dopaminergic interneurons, particularly in the GL [37-39]. In accordance, TH was observed in large cell bodies in the glomerular periphery and in their varicose axons projecting to the adjacent GLu. Some TH positive neurons processes extended to two or three glomeruli. In this sense, the existence of "*transglomerular*" neurons, likely dopaminergic/GABAergic neurons were reported [39,40]. In DOCA-Salt rats the axonal branching of catecholaminergic neurons in the OB (defined as the positive area in the GLu) was three-fold higher than in normotensive rats and further the immnopositive area was lower in the PG area suggesting a focal distribution of the neuritis in the GLu. Conversely, in both hypertensive and normotensive animals the fluorescence intensity (indicative of TH amount) was higher in the PG area, reflecting TH accumulation within the neuronal cell bodies. Hypertensive rats showed higher TH content in both GLu and PG area supporting that DOCA-Salt rats express higher TH levels than controls. These findings correlated well with TH expression assessed by immunoblotting in the present and previous studies [14]. Higher TH expression and activity supports enhanced sympathetic outflow.

Both ET receptor subtypes are present in the brain, including the OB, but their distribution in experimental models of hypertension has not been yet investigated. We here show that, in the GL of the OB, ET_A receptor was mainly found in the GLu. Fluorescence was dispersed

and appeared to follow neuronal axons. Additionally, in the PG area small cells showing ET_A immunoreactivity were also observed. Although ET_A distribution in the OB of normotensive and hypertensive rats followed the same pattern, hypertensive rats showed enhanced immunofluorescence intensity in the Glu. These findings suggest that ET_A is overexpressed in nerve fibers that integrate sensitive information. The significant increase in ET_A/TH co-localization in DOCA-Salt rats is likely related to the modulation of TH activity by ETs signaling through ET_A. It was surprising that hypertensive rats did not exhibit increased ET_A/TH co-localization in the PG area, which would relate to a similar modulation of catecholaminergic activity by ETs in neuronal cell bodies. Nevertheless, given that TH is the rate liming enzyme in catecholamine biosynthesis which occurs in varicosities and axon terminals, increased co-localization supports a relevant role of ETs in the modulation of catecholamine transmission.

The distribution of ET_B receptors in the brain has been less studied but it was reported that its mRNA expression is higher than that of ET_A [42,43]. In the present study, the percentage of ET_B immunoreactive area was higher in the GLu than in the PG area, while the intensity showed opposite distribution, in both normotensive and hypertensive animals. Hypertensive rats were only different in that the distribution of the immunopositive area in the GLu was lower. The apparent discrepancy regarding the expression of ET_B assessed by western blot and quantitative RT-PCR may arise from the different regions assessed with each technique. Nevertheless, as the ET_B receptor is associated with blood pressure lowering, the decrease of this receptor subtype in hypertensive animals is not surprising.

ET receptors and catecholamines have been found in similar brain regions such as the locus coeruleus, hypothalamus, amygdala and the GL of the OB [44–46]. To the best of our knowledge this is the first study to report in rats that ET receptors co-localize with TH in the GL of OB and that this co-localization is enhanced in hypertensive rats. In previous studies we showed that ET-1 increases TH expression in the OB and that the enzyme activity and expression is higher in DOCA-Salt rats [14,23]. Given that DOCA-Salt rats show high ET-1 levels in the CSF, our results support endogenous overstimulation of ET_A in the OB, leading to enhanced brain catecholaminergic activity, which may in turn directly or indirectly induce chronic blood pressure elevation.

In the present work, following ETA blockade, SBP in hypertensive rats was significantly reduced (approximately 20 mmHg). Previous studies show that centrally applied ETs to normotensive animals increases blood pressure through ETA activation causing enhanced sympathetic outflow and arginine-vasopressin activity [45,47,48]. In DOCA-salt hypertension the degree of sympathetic overflow correlates with the level of ETs in both plasma and CSF. In this sense, the endothelinergic system is considered a key factor in salt-dependent hypertension associated with a sympathetic overflow [30,46,49,50]. In spontaneously hypertensive rats, centrally applied ET_A antagonists reduce blood pressure, and nerve sympathetic activity [49]. Furthermore, ETA or ETA/ETB antagonists applied to the periaqueductal grey area, decrease blood pressure [32]. It was also shown that ETs stimulate catecholamine release from nerve endings and regulate cardiovascular function through sympathetic activation [45,46]. Likewise, we previously reported that ETs regulate noradrenergic transmission in the posterior and anterior rat hypothalamus in normotensive

and DOCA-Salt rats [33,51,52]. Previous and present findings strongly support that the brain endothelinergic system regulates cardiovascular activity through an ETA-mediated sympathoexcitatory response and further suggest that this may contribute to maintain blood pressure chronically elevated.

Hypertensive animals showed higher TH activity and expression in the OB than normotensive rats as previously reported [14]. DOCA-Salt rats show alterations in the brain endothelinergic system and, also, the central administration of ETs increases catecholaminergic activity in the OB. In accordance, we observed that hypertensive rats expressed higher ET_A expression and ET_A/TH co-localization, and further that ET_A blockade decreased TH activity and expression. The increase in TH activity and expression in the OB would be a long-term response sustained by ETs up-regulation. These peptides activate various transcription factors, some of which bind to the promotor region of the TH gene [53–55]. In this sense, preliminary studies from our laboratory show that ET-1 and ET-3 increase CREB and c-fos expression in the OB of normotensive rats. Taken together, these findings would explain the higher increase in TH mRNA in the OB of hypertensive rats.

An interesting finding was that acute ET_A blockade decreased TH mRNA and protein to control levels. The short exposure to the ET_A antagonist, suggested the activation of a TH degrading mechanism. Degradation of TH occurs through different mechanisms including lysosomal and chymotrypsin pathways, but the major route is the ubiquitin-proteasome system [35,56–58]. Proteasome inhibition induced no changes in blood pressure or heart rate either in normotensive or hypertensive animals, but it prevented the hypotensive effect of BQ610 in DOCA-Salt rats. MG132 administration augmented TH activity in the OB of normotensive rats but considering that the enzyme is equally active in normotensive animals treated with vehicle or MG132+BQ610, and less with MG132 alone, proteasome inhibition would evidence that the antagonist forces the response reducing the activity of the enzyme. The expression of total TH and its phosphorylated forms were in line with this consideration. Proteasome inhibition significantly increased TH-PSer19 and TH mRNA, that were not reflected on TH protein content likely due to the short time exposure [59,60]. The ubiquitin-proteasome system is also in the cell nucleus where it not only degrades proteins, but it also regulates mRNA levels. Thus, proteasome inhibition affects mRNA stability and its translocation to the cytoplasm among other reported functions [56,58]. TH linked to ubiquitin showed not changes in normotensive animals, in line with TH protein expression. In hypertensive rats, proteasome inhibition did not affect TH. Early studies reported that DOCA-Salt hypertensive rats exhibited higher proteasome content and activity than normotensive animals. Accordingly, we showed that hypertensive rats were more sensible to proteasome inhibition. A recent report showed in multiple myeloma cells that ET-1 through ET_B receptors induces proteasome overregulation which confers resistance to inhibitory agents [61]. These findings, and the fact that DOCA-Salt rats show higher ET-1 levels in the CSF, would explain the finding that MG132 alone had no effect on TH activity in these animals. In accordance, proteasome inhibition did not modify the expression of total TH or its phosphorylated forms, except for TH-PSer31. Given that the ubiquitin-proteasome system degrades mainly TH phosphorylated at Ser 19 and Ser40 sites, the implication of this finding is presently unknown [56,60]. Blockade of ET_A reduced TH activity in hypertensive

animals which was prevented by MG132. A similar behavior was observed when the phosphorylated forms of the enzyme or TH mRNA were assessed. In summary, these observations suggest that proteasome inhibition would contribute to ET_A blockade response in hypertensive rats.

Proteasome inhibition induced a slight increase (27%) in ubiquitin-linked TH in the OB of hypertensive animals in line with decreased proteasome activity. However, concomitant ET_A blockade induced a significant accumulation of ubiquitin-TH (51%). Given the basal proteasome activity, the level of ubiquitin-TH in DOCA-Salt rats, and the steady state of this system in the OB, a disruption like an ET_A receptor blockade, may accumulate a higher amount of ubiquitin-TH. However, as BQ610 was acutely administered, it is likely that the system fails to compensate the destabilization in response to ET_A blockade, increasing ubiquitin-TH. Additionally, ET_A blockade may enhance ET-1 local concentration, triggering ET_B activation, which, in turn, may up-regulate the proteasome activity [61]. Taken together, the amount of a protein linked to ubiquitin would result from the kinetics of each reaction and the underlying signal transduction pathways.

Though not fully understood, evidence strongly supports a close relationship between the OB and the cardiovascular function. Changes in the vascular and cardiac function impact on various neurotransmitters including catecholamines in the OB [6]. The integrity of OB is crucial to elicit a normal excitatory response to physiological stimuli and their bilateral removal modifies blood pressure and heart rate [2,3,18]. Unpublished observations from our laboratory show that bilateral bulbectomy diminishes systolic blood pressure in DOCA-Salt rats but not in normotensive animals. Furthermore, BQ610 applied to the OB of DOCA-Salt animals diminishes systolic blood pressure as observed in the present study.

The OB connect with major brain areas involved in the regulation of cardiovascular function. The main OB projects to the piriform cortex, amygdala and entorhinal cortex, whereas the accessory OB projects to the dorsal olfactory tract, amygdala and stria terminalis. In turn, some of these regions connect with the posterior and anterior hypothalamus as well as the preoptic area [6,18,25]. Findings suggest that the endothelinergic system in the OB may play a relevant role in the central regulation of cardiovascular function through the sympathetic nervous system in health and disease.

To our knowledge, there are no reports in the literature that relate smell to salt intake in animal models of hypertension. An interesting finding is that the olfactory mucosa expresses high affinity mineralocorticoid receptors [62]. It was also shown that the loss of olfactory performance can be a consequence of the lack of sodium [63]. These data suggest a relationship between smell, sodium intake and cardiovascular function.

In summary, the present study advances in the knowledge of the central mechanisms involved in DOCA-Salt hypertension, focusing on the regulation of catecholamines by ETs in the OB. Figure 9 depicts the proposed mechanism. The higher expression of ET_A in the olfactory glomeruli of hypertensive rats would enhance TH expression and activity thus leading in a direct or indirect way to sympathetic overflow and hypertension. The acute ET_A blockade reveals the relevance of this mechanism in the maintenance of chronic blood

pressure elevation. Present findings give further support to the role of the OB in the regulation of cardiovascular function in hypertension. Increasing evidence supports an association between the OB and cardiovascular impairment. The loss of smell in humans correlates with higher salt intake, which enhances the risk of hypertension. Furthermore, a close relationship exists between cardiovascular diseases and depression, and further depression and the OB. In this context, our results support the relevance of the OB in the regulation of chronic blood pressure elevation and the strong contribution of endothelins. New insights into the pathophysiological mechanisms underlying salt-dependent hypertension may help to design new strategies or drugs for this disease which is a major global health concern.

Acknowledgement

We thank Mónica Navarro and Gabriela Nocetti for their excellent technical assistance.

Grant support list

This work was supported by CONICET grant PIP 112-201101-00570 (MSV and LGB), ANPCyT grant PICT 2015-2030 (MSV), UBA grant UBACyT 20020100100695 (MSV and LGB) and NIH R01HL112225 (JS). Some of the experiments were carried out under a grant funded by the Bunge and Born Foundation and the Fulbright Commission (MJG).

5. References

[1]. Dampney RAL, Central neural Control of the cardiovascular system: current perspectives, Adv. Physiol. Educ. 40 (2016) 283–296. 10.1152/advan.00027.2016 [PubMed: 27445275]

[2]. Grippo AJ, Johnson AK, Stress, depression and cardiovascular dysregulation: a review of neurobiological mechanisms and the integration of research from preclinical disease models., Stress. 12 (2009) 1–21. 10.1080/10253890802046281 [PubMed: 19116888]

[3]. Kawasaki H, Watanabe S, Ueki S, Changes in blood pressure and heart rate following bilateral olfactory bulbectomy in rats., Physiol. Behav. 24 (1980) 51–56. 10.1016/0031-9384(80)90013-X. [PubMed: 7189889]

[4]. Moffitt JA, Grippo AJ, Holmes PV, Johnson AK, Olfactory bulbectomy attenuates cardiovascular sympathoexcitatory reflexes in rats., Am. J. Physiol. Heart Circ. Physiol. 283 (2002) H2575–2583. 10.1152/ajpheart.00164.2002 [PubMed: 12388291]

[5]. Kawasaki H, Watanabe S, Ueki S, Potentiation of pressor and behavioral responses to brain stimulation following bilateral olfactory bulbectomy in freely moving rats., Brain Res. Bull. 5 (1980) 711 10.1016/0361-9230(80)90210-5 [PubMed: 7193505]

[6]. Kelly JP, Wrynn AS, Leonard BE, The olfactory bulbectomized rat as a model of depression: an update., Pharmacol. Ther. 74 (1997) 299–316. 10.1016/S0163-7258(97)00004-1 [PubMed: 9352586]

[7]. Bader A, Klein B, Breer H, Strotmann J, Connectivity from OR37 expressing olfactory sensory neurons to distinct cell types in the hypothalamus, Front. Neural Circuits. 6 (2012) 84 10.3389/fncir.2012.00084 [PubMed: 23162434]

[8]. Takahashi LK, Sullivan RM, Rosen JB, Olfactory systems and neural circuits that modulate predator odor fear, 8 (2014) 72 10.3389/fnbeh.2014.00072

[9]. Nagai K, Niijima A, Horii Y, Shen J, Tanida M, Olfactory stimulatory with grapefruit and lavender oils change autonomic nerve activity and physiological function., Auton. Neurosci. 185 (2014) 29–35. 10.1016/j.autneu.2014.06.005 [PubMed: 25002406]

[10]. Allen W, Olfactory and trigeminal conditioned reflexes in dogs, Am. J. Physiol. Content. 118 (1937) 532–540. 10.1152/ajplegacy.1937.118.3.532

[11]. Nakamura T, Hayashida Y, Autonomic cardiovascular responses to smoke exposure in conscious rats., Am. J. Physiol. 262 (1992) R738–745. 10.1152/ajpregu.1992.262.5.R738 [PubMed: 1590469]

[12]. Nagai M, Wada M, Usui N, Tanaka A, Hasebe Y, Pleasant odors attenuate the blood pressure increase during rhythmic handgrip in humans., Neurosci. Lett. 289 (2000) 227–229. 10.1016/S0304-3940(00)01278-7 [PubMed: 10961671]

[13]. Shen J, Niijima A, Tanida M, Horii Y, Maeda K, Nagai K, Olfactory stimulation with scent of lavender oil affects autonomic nerves, lipolysis and appetite in rats., Neurosci. Lett. 383 (2005) 188–193. 10.1016/j.neulet.2005.04.010 [PubMed: 15878236]

[14]. Abramoff T, Guil MJ, Morales VP, Hope SI, Soria C, Bianciotti LG, Vatta MS, Enhanced assymetrical noradrenergic transmission in the olfactory bulb of deoxycorticosterone acetate-salt hypertensive rats., Neurochem. Res. 38 (2013) 2063–2071. 10.1007/s11064-013-1114-0 [PubMed: 23888389]

[15]. Kiecolt-Glaser JK, Graham JE, Malarkey WB, Porter K, Lemeshow S, Glaser R, Olfactory influences on mood and autonomic, endocrine, and immune function., Psychoneuroendocrinology. 33 (2008) 328–339. 10.1016/j.psyneuen.2007.11.015 [PubMed: 18178322]

[16]. Köteles F, Babulka P, Role of expectations and pleasantness of essential oils in their acute effects., Acta Physiol. Hung. 101 (2014) 329–340. 10.1556/APhysiol.101.2014.3.8 [PubMed: 25183507]

[17]. Pohorecky LA, Zigmond MJ, Heimer L, Wurtman RJ, Olfactory bulb removal: effects on brain norepinephrine., Proc. Natl. Acad. Sci. U. S. A. 62 (1969) 1052–1055. 10.1073/pnas.62.4.1052 [PubMed: 5256405]

[18]. Song C, Leonard BE, The olfactory bulbectomised rat as a model of depression, Neurosci. Biobehav. Rev. 29 (2005) 627–647. 10.1016/j.neubiorev.2005.03.010. [PubMed: 15925697]

[19]. Maturana MJ, Pudell C, Targa ADS, Rodrigues LS, Noseda ACD, Fortes MH, Dos Santos P, Da Cunha C, Zanata SM, Ferraz AC, Lima MMS, REM sleep deprivation reverses neurochemical and other depressive-like alterations induced by olfactory bulbectomy., Mol. Neurobiol. 51 (2015) 349–360. 10.1007/s12035-014-8721-x [PubMed: 24826915]

[20]. Thakare VN, Aswar MK, Kulkami YP, Patil RR, Patel BM, Silymarin ameliorates experimentally induced depressive like behavior in rats: Involvement of hippocampal BDNF signaling, inflammatory cytokines and oxidative stress response, Physiol. Behav. 179 (2017) 401–410. 10.1016/j.physbeh.2017.07.010 [PubMed: 28711395]

[21]. Kohzuki M, Chai SYY, Paxinos G, Karavas A, Casley DJJ, Johnston CII, Mendelsohn FAOA, Localization and characterization of endothelin receptor binding sites in the rat brain visualized by in vitro autoradiography4, Neuroscience. 42 (1991) 245–260. 10.1016/0306-4522(91)90162-H [PubMed: 1650432]

[22]. Warner TD, Budzik GP, Matsumoto T, Mitchell JA, Förstermann U, Murad F, Regional differences in endothelin converting enzyme activity in rat brain: inhibition by phosphoramidon and EDTA., Br. J. Pharmacol. 106 (1992) 948–952. 10.1111/j.1476-5381.1992.tb14440.x [PubMed: 1393292]

[23]. Nabhen SL, Morales VP, Guil MJ, Höcht C, Bianciotti LG, Vatta MS, Mechanisms involved in the long-term modulation of tyrosine hydroxylase by endothelins in the olfactory bulb of normotensive rats., Neurochem. Int. 58 (2011) 196–205. 10.1016/j.neuint.2010.11.016 [PubMed: 21129429]

[24]. Nabhen SL, Guil MJ, Saffioti N, Morales VP, Bianciotti LG, Vatta MS, Calcium-dependent mechanisms involved in the modulation of tyrosine hydroxylase by endothelins in the olfactory bulb of normotensive rats., Neurochem. Int. 62 (2013) 389–398. 10.1016/j.neuint.2013.01.018 [PubMed: 23357475]

[25]. Oparil S, Chen Y-F, Berecek K, Calhoun D, Wyss J, Oparil J, Chen Y-F, Berecek K, Calhoun D, Wyss S, Oparil S, Chen Y-F, Berecek K, Calhoun D, Wyss J, Oparil J, Chen Y-F, Berecek K, Calhoun D, Wyss S, The role of the Central Nervous System in Hypertension, in: Hypertens. Pathophysiol. Diagnosis Manegment, Second, 1995: pp. 713–739.

[26]. Basting T, Lazartigues E, DOCA-Salt Hypertension: an Update, Curr. Hypertens. Rep. 19 (2017) 32 10.1007/s11906-017-0731-4 [PubMed: 28353076]

[27]. Khor S, Cai D, Hypothalamic and inflammatory basis of hypertension, Clin. Sci. 131 (2017) 211–223. 10.1042/CS20160001 [PubMed: 28057892]

[28]. de Morais SDB, Shanks J, Zucker IH, Integrative Physiological Aspects of Brain RAS in Hypertension, Curr. Hypertens. Rep. 20 (2018) 10 10.1007/s11906-018-0810-1 [PubMed: 29480460]

[29]. Parati G, Esler M, The human sympathetic nervous system: Its relevance in hypertension and heart failure, Eur. Heart J. 33 (2012) 1058–1066. 10.1093/eurheartj/ehs041 [PubMed: 22507981]

[30]. Yemane H, Busauskas M, Burris SK, Knuepfer MM, Neurohumoral mechanisms in deoxycorticosterone acetate (DOCA)-salt hypertension in rats., Exp. Physiol. 95 (2010) 51–55. 10.1113/expphysiol.2008.046334 [PubMed: 19700514]

[31]. Naruse M, Takagi S, Tanabe A, Naruse K, Adachi C, Yoshimoto T, Seki T, Takano K, Augmented expression of tissue endothelin-1 messenger RNA is a common feature in hypertensive rats., J. Cardiovasc. Pharmacol. 36 (2000) S195–S197. 10.1097/00005344-200036001-00059 [PubMed: 11078375]

[32]. Di Filippo C, D'Amico M, Piegari E, Rinaldi B, Filippelli A, Rossi F, Local administration of ET_A (but not ET_B) blockers into the PAG area of the brain decreases blood pressure of DOCA-salt rats., Naunyn. Schmiedebergs. Arch. Pharmacol. 366 (2002) 123–126. 10.1007/s00210-002-0566-6 [PubMed: 12122498]

[33]. Abramoff T, Guil MJ, Morales VP, Hope SI, Höcht C, Bianciotti LG, Vatta MS, Involvement of endothelins in deoxycorticosterone acetate-salt hypertension through the modulation of noradrenergic transmission in the rat posterior hypothalamus., Exp. Physiol. 100 (2015) 617–627. 10.1113/EP085230 [PubMed: 25809871]

[34]. Cassinotti LR, Guil MJ, Schöller MI, Navarro MP, Bianciotti LG, Vatta MS, Chronic Blockade of Brain Endothelin Receptor Type-A (ET_A) Reduces Blood Pressure and Prevents Catecholaminergic Overactivity in the Right Olfactory Bulb of DOCA-Salt Hypertensive Rats., Int. J. Mol. Sci. 19 (2018) 660 10.3390/ijms19030660

[35]. Carbajosa NAL, Corradi G, Verrilli MAL, Guil MJ, Vatta MS, Gironacci MM, Gironacci MM, Tyrosine Hydroxylase Is Short-Term Regulated by the Ubiquitin- Proteasome System in PC12 Cells and Hypothalamic and Brainstem Neurons from Spontaneously Hypertensive Rats: Possible Implications in Hypertension, PLoS One. 10 (2015) e0116597 10.1371/journal.pone.0116597 [PubMed: 25710381]

[36]. Reinhard JF, Smith GK, Nichol CA, A rapid and sensitive assay for tyrosine-3- monooxygenase based upon the release of 3H2O and adsorption of [3H]-tyrosine by charcoal., Life Sci. 39 (1986) 2185–2189. 10.1016/0024-3205(86)90395-4 [PubMed: 2878337]

[37]. Kosaka T, Kosaka K, Structural Organization of the Glomerulus in the Main Olfactory Bulb, Chem. Senses. 30 (2005) i107–i108. 10.1093/chemse/bjh137 [PubMed: 15738062]

[38]. Nagayama S, Homma R, Imamura F, Neuronal organization of olfactory bulb circuits., Front. Neural Circuits. 8 (2014) 98 10.3389/fncir.2014.00098 [PubMed: 25232305]

[39]. Toida K, Kosaka K, Aika Y, Kosaka T, Chemically defined neuron groups and their subpopulations in the glomerular layer of the rat main olfactory bulb-IV. Intraglomerular synapses of tyrosine hydroxylase-immunoreactive neurons, Neuroscience. 101 (2000) 11–17. 10.1016/S0306-4522(00)00356-0 [PubMed: 11068132]

[40]. Kosaka T, Kosaka K, Neuronal organization of the main olfactory bulb revisited, Anat. Sci. Int. 91 (2016) 115–127. 10.1007/s12565-015-0309-7 [PubMed: 26514846]

[41]. Meiners S, Dreger H, Fechner M, Bieler S, Rother W, Günther C, Baumann G, Stangl V, Stangl K, Suppression of cardiomyocyte hypertrophy by inhibition of the ubiquitin-proteasome system., Hypertension. 51 (2008) 302–308. 10.1161/HYPERTENSIONAHA.107.097816 [PubMed: 18086945]

[42]. Davenport AP, Hyndman KA, Dhaun N, Southan C, Kohan DE, Pollock JS, Pollock DM, Webb DJ, Maguire JJ, Endothelin, Pharmacol. Rev. 68 (2016) 357–418. 10.1124/pr.115.011833 [PubMed: 26956245]

[43]. Kurokawa K, Yamada H, Ochi J, Topographical distribution of neurons containing endothelin type A receptor in the rat brain., J. Comp. Neurol. 389 (1997) 348–360. 10.1002/(SICI)1096-9861(19971215)389:2<348::AID-CNE11>3.0.CO;2-H [PubMed: 9416926]

[44]. Sluck JM, Lin RCS, Katolik LI, Jeng AY, Lehmann JC, Endothelin converting enzyme-1-, endothelin-1-, and endothelin-3-like immunoreactivity in the rat brain, Neuroscience. 91 (1999) 1483–1497. 10.1016/S0306-4522(98)00692-7 [PubMed: 10391453]

[45]. Kuwaki T, Kurihara H, CAO WH, Kurihara Y, Unekawa M, YAZAKI Y, Kumada M, Physiological role of brain endothelin in the central autonomic Control: from neuron to knockout mouse., Prog. Neurobiol. 51 (1997) 545–579. 10.1016/S0301-0082(96)00063-9 [PubMed: 9153073]

[46]. Kohan DE, Rossi NF, Inscho EW, Pollock DM, Regulation of blood pressure and salt homeostasis by endothelin., Physiol. Rev. 91 (2011) 1–77. 10.1152/physrev.00060,2009 [PubMed: 21248162]

[47]. Chen A-D, Xiong X-Q, Gan X-B, Zhang F, Zhou Y-B, Gao X-Y, Han Y, Endothelin-1 in paraventricular nucleus modulates cardiac sympathetic afferent reflex and sympathetic activity in rats., PLoS One. 7 (2012) e40748 10.1371/journal.pone.0040748 [PubMed: 22815806]

[48]. Dhaun N, Goddard J, Kohan DE, Pollock DM, Schiffrin EL, Webb DJ, Role of endothelin-1 in clinical hypertension: 20 years on, 52 (2008) 452–459. 10.1161/HYPERTENSIONAHA.108.117366

[49]. Nakamura K, Sasaki S, Moriguchi J, Morimoto S, Miki S, Kawa T, Itoh H, Nakata T, Takeda K, Nakagawa M, Central effects of endothelin and its antagonists on sympathetic and cardiovascular regulation in SHR-SP., J. Cardiovasc. Pharmacol. 33 (1999) 876–882. 10.1097/00005344-199906000-00007 [PubMed: 10367590]

[50]. Zicha J, Dobešova Z, Vokurková M, Rauchová H, Hojná S, Kadlecová M, Behuliak M, Vaněčková I, Kuneš J, Age-dependent salt hypertension in Dahl rats: fifty years of research., Physiol. Res. 61 Suppl 1 (2012) S35–87. http://www.ncbi.nlm.nih.gov/pubmed/22827876 (accessed June 13, 2017). [PubMed: 22827876]

[51]. di Nunzio AS, Jaureguiberry MS, Rodano V, Bianciotti LG, Vatta MS, Endothelin-1 and -3 diminish neuronal NE release through an NO mechanism in rat anterior hypothalamus., Am. J. Physiol. Regul. Integr. Comp. Physiol. 283 (2002) R615–22. 10.1152/ajpregu.00026.20Q2 [PubMed: 12184995]

[52]. Perfume G, Nabhen SL, Barrera KR, Otero MG, Bianciotti LG, Vatta MS, Otero G, Long-term modulation of tyrosine hydroxylase activity and expression by endothelin-1 and -3 in the rat anterior and posterior hypothalamus., Am. J. Physiol. Regul. Integr. Comp. Physiol. 294 (2008) R905–14. 10.1152/ajpregu.00555.2007 [PubMed: 18094067]

[53]. Gras E, Belaidi E, Briançon-Marjollet A, Pépin J-L, Amaud C, Godin-Ribuot D, Endothelin-1 mediates intermittent hypoxia-induced inflammatory vascular remodeling through HIF-1 activation., J. Appl. Physiol. 120 (2016) 437–443. 10.1152/japplphysiol.00641.2015 [PubMed: 26679613]

[54]. Lenartowski R, Goc A, Epigenetic, transcriptional and posttranscriptional regulation of the tyrosine hydroxylase gene., Int. J. Dev. Neurosci. 29 (2011) 873–883. 10.1016/j.ijdevneu.2011.07.006 [PubMed: 21803145]

[55]. Morawietz H, Wagner AH, Hecker M, Goettsch W, Endothelin receptor B-mediated induction of c-jun and AP-1 in response to shear stress in human endothelial cells., Can. J. Physiol. Pharmacol. 86 (2008) 499–504. 10.1139/Y08-026 [PubMed: 18758496]

[56]. Nakashima A, Kodani Y, Kaneko YS, Nagasaki H, Ota A, Proteasome-mediated degradation of tyrosine hydroxylase triggered by its phosphorylation: a new question as to the intracellular location at which the degradation occurs, J. Neural Transm. 125 (2016) 9–15. 10.1007/s00702-016-1653-z [PubMed: 27866280]

[57]. Tank AW, Xu L, Chen X, Radcliffe P, Sterling CR, Post-transcriptional regulation of tyrosine hydroxylase expression in adrenal medulla and brain., Ann. N. Y. Acad. Sci. 1148 (2008) 238–248.10.1196/annals.1410.054 [PubMed: 19120116]

[58]. Yao T, Ndoja A, Regulation of gene expression by the ubiquitin-proteasome system, Semin. Cell Dev. Biol. 23 (2012) 523–529. 10.1016/j.semcdb.2012.02.006 [PubMed: 22430757]

[59]. Kawahata I, Ohtaku S, Tomioka Y, Ichinose H, Yamakuni T, Dopamine or biopterin deficiency potentiates phosphorylation at 40Ser and ubiquitination of tyrosine hydroxylase to be degraded by the ubiquitin proteasome system, Biochem. Biophys. Res. Commun. 465 (2015) 53–58. 10.1016/j.bbrc.2015.07.125 [PubMed: 26225746]

[60]. Tekin I, Roskoski R, Carkaci-Salli N, Vrana KE, Complex molecular regulation of tyrosine hydroxylase., J. Neural Transm. 121 (2014) 1451–1481. 10.1007/s00702-014-1238-7 [PubMed: 24866693]

[61]. Vaiou M, Pangou E, Liakos P, Sakellaridis N, Vassilopoulos G, Dimas K, Papandreou C, Endothelin-1 (ET-1) induces resistance to bortezomib in human multiple myeloma cells via a pathway involving the ET_B receptor and upregulation of proteasomal activity, J. Cancer Res. Clin. Oncol. 142 (2016) 2141–2158. 10.1007/s00432-016-2216-2 [PubMed: 27530445]

[62]. Kern RC, Foster JD, Pitovski DZ, Mineralocorticoid (type I) receptors in the olfactory mucosa of the mammal: studies with [3H]aldosterone and the anti-mineralocorticoid spironolactone., Chem. Senses. 22 (1997) 141–148. 10.1093/chemse/22.2.141 [PubMed: 9146904]

[63]. Weiler E, Deutsch S, Apfelbach R, Combined behavioral and c-Fos studies elucidate the vital role of sodium for odor detection., Chem. Senses. 31 (2006) 641–647. 10.1093/chemse/bjl004 [PubMed: 16804091]

Highlights

- The pathophysiological mechanisms underlying hypertension still remain unclear but brain endothelins are thought to play a key role;
- Increasing evidence supports an association between the olfactory bulb and cardiovascular impairment;
- Enhanced endothelin type A receptors and colocalization with tyrosine hydroxylase in olfactory bulbs occurs in DOCA-salt hypertension;
- Blockade of endothelin type A receptors results in the decrease of blood pressure and accelerated tyrosine hydroxylase degradation;
- The interaction of endothelins and catecholamines in the olfactory bulbs would contribute to the genesis of salt-dependent hypertension.

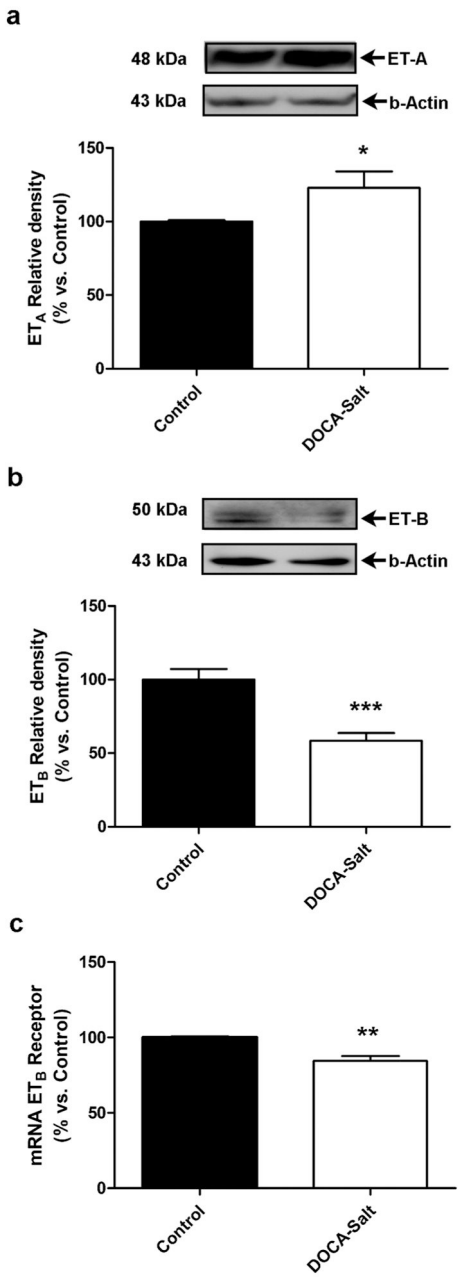

Figure 1: Expression of endothelin receptors, ET_A and ET_B, in the olfactory bulb of normotensive and DOCA-Salt hypertensive rats.

(a) Representative western blots and densitometric analysis for ET_A expression in the olfactory bulb of Control and DOCA-Salt rats, **(b)** Representative western blots and densitometric analysis for ET_B expression in the olfactory bulb of Control and DOCA-Salt rats, **(c)** ET_B mRNA expression in the olfactory bulb of Control and DOCA-Salt assessed by real time RT-PCR as detailed in Materials and Methods. * $p<0.05$; ** $p<0.01$; *** $p<0.001$ vs. Control. Number of animals per experimental group: 5.

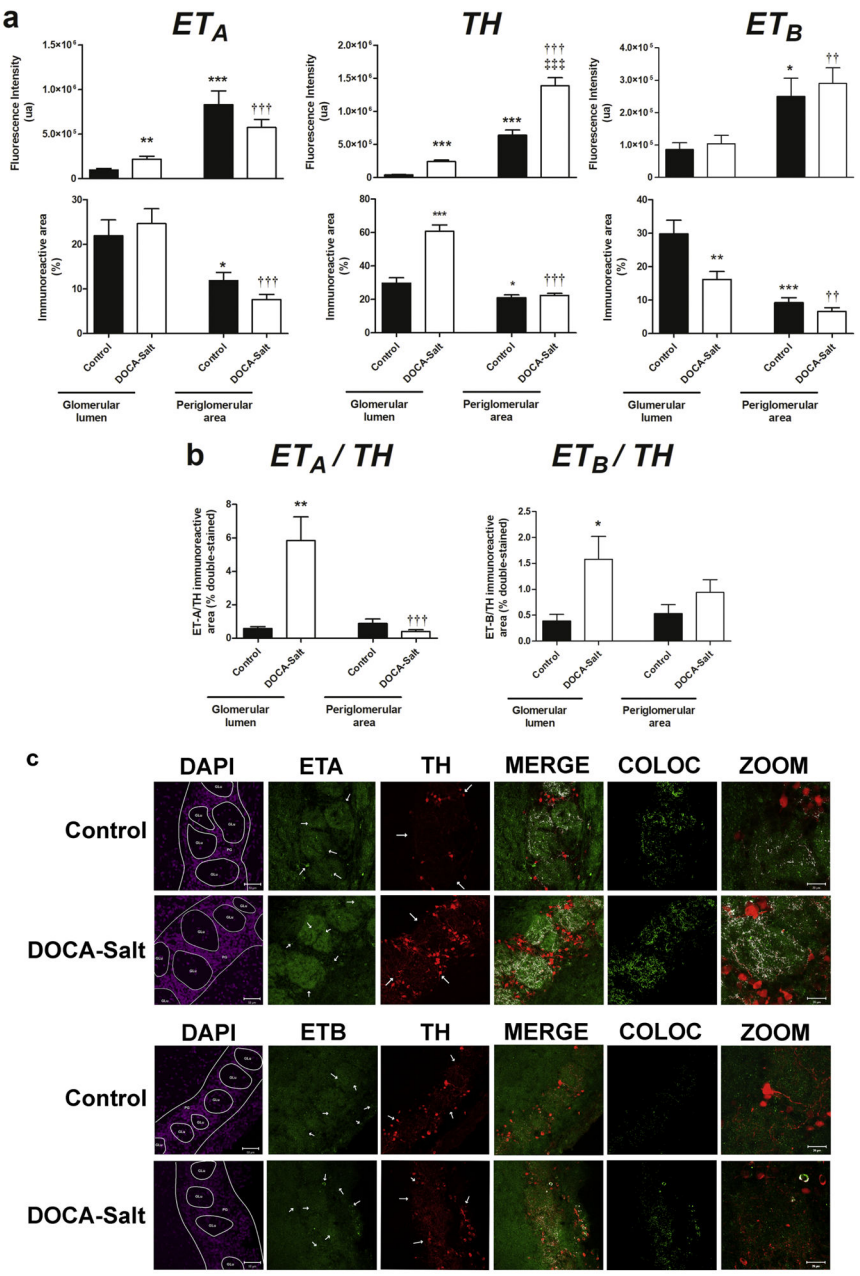

Figure 2: Expression, distribution and co-localization of endothelin receptors (ET_A and ET_B) and tyrosine hydroxylase (TH) in the glomerular layer of the olfactory bulb of normotensive and DOCA-Salt hypertensive rats.

Endothelin receptors and TH were assessed in the glomerular lumen and the periglomerular area of the olfactory bulb by confocal microscopy as detailed in Materials and Methods. Incubations were performed with a triple staining: ET_A/TH/DAPI or ET_B/TH/DAPI. DAPI images were used to determine the glomeruli lumen and to discriminate the glomerular layer from other olfactory bulb layers. **(a)** Quantifications corresponding to total fluorescence intensity and percentage of immunopositive areas for ET_A, TH and ET_B. The quantification was performed with the Image J software in the stack of the images set, always limiting the

measurement to the threshold value of each set of images. **(b)** Quantification of the co-localization of ET_A/TH or ET_B/TH expressed as percentage of the double-immunopositive area. Using an Image J plugin for co-localization measurement and the threshold value for the images previously calculated two images were generated with colocalization information: one with the double staining and the co-localized pixels marked in white, and another one only with the co-localized pixels depicted. The later was quantified to evaluate the percentage of the double-immunopositive area **(c)** Representative images for DAPI, ET_A (uppers rows), ET_B (lower rows) and TH. Colocalization is shown in white (MERGE). COLOC: Colocalization 8-bit image from the colocalization analysis); ZOOM: images acquired with a 2.8X optic zoom to further discriminate the colocalization of ETA/TH or ETB/TH in the OB. Arrow heads show immunopositive fibers or cell bodies. *: $p<0.05$, **: $p<0.01$, ***: $p<0.001$ *vs.* Control (glomerular lumen); ††: $p<0.01$, †††: $p<0.001$ *vs.* DOCA-salt (glomerular lumen); ‡‡‡ $p<0.001$ *vs.* Control (periglomerular area). Number of animals per experimental group: 5

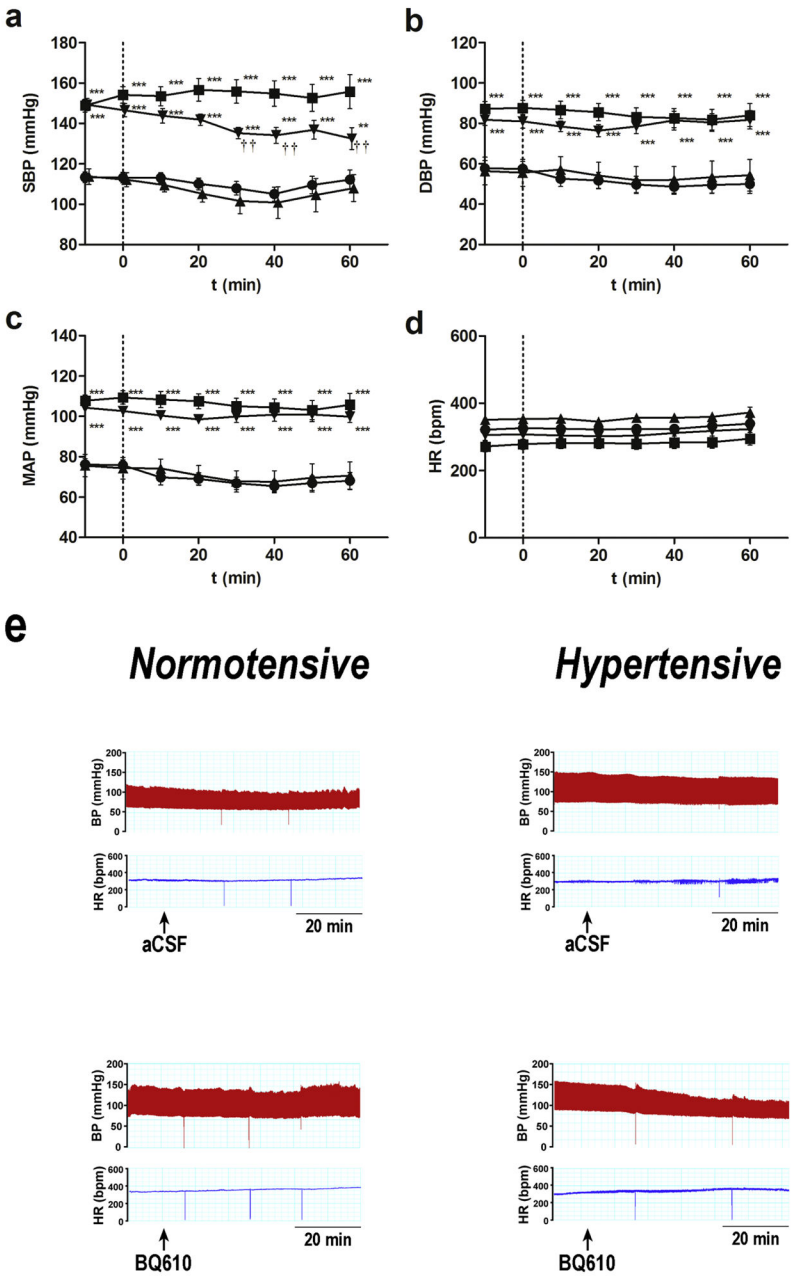

Figure 3: Hemodynamic parameters following ET_A blockade by BQ610 in normotensive and DOCA-Salt hypertensive rats.

Time course (a) systolic blood pressure (SBP), (b) diastolic blood pressure (DBP), (c) mean arterial pressure (MAP) and heart rate (HR) following BQ610 (20 μM) administration to normotensive (control) and hypertensive (DOCA-Salt) animals as detailed in Materials and Methods. (e) Representative traces of blood pressure and HR following ETA blockade. ●: Control; ■: DOCA-Salt; ▲: Control+BQ610; ▼: DOCA-Salt+BQ610. **: p<0.01, ***: p<0.001 *vs.* Control+aCSF; ††: p<0.01 *vs.* DOCA-Salt+aCSF. Number of animals per experimental group: 15-19.

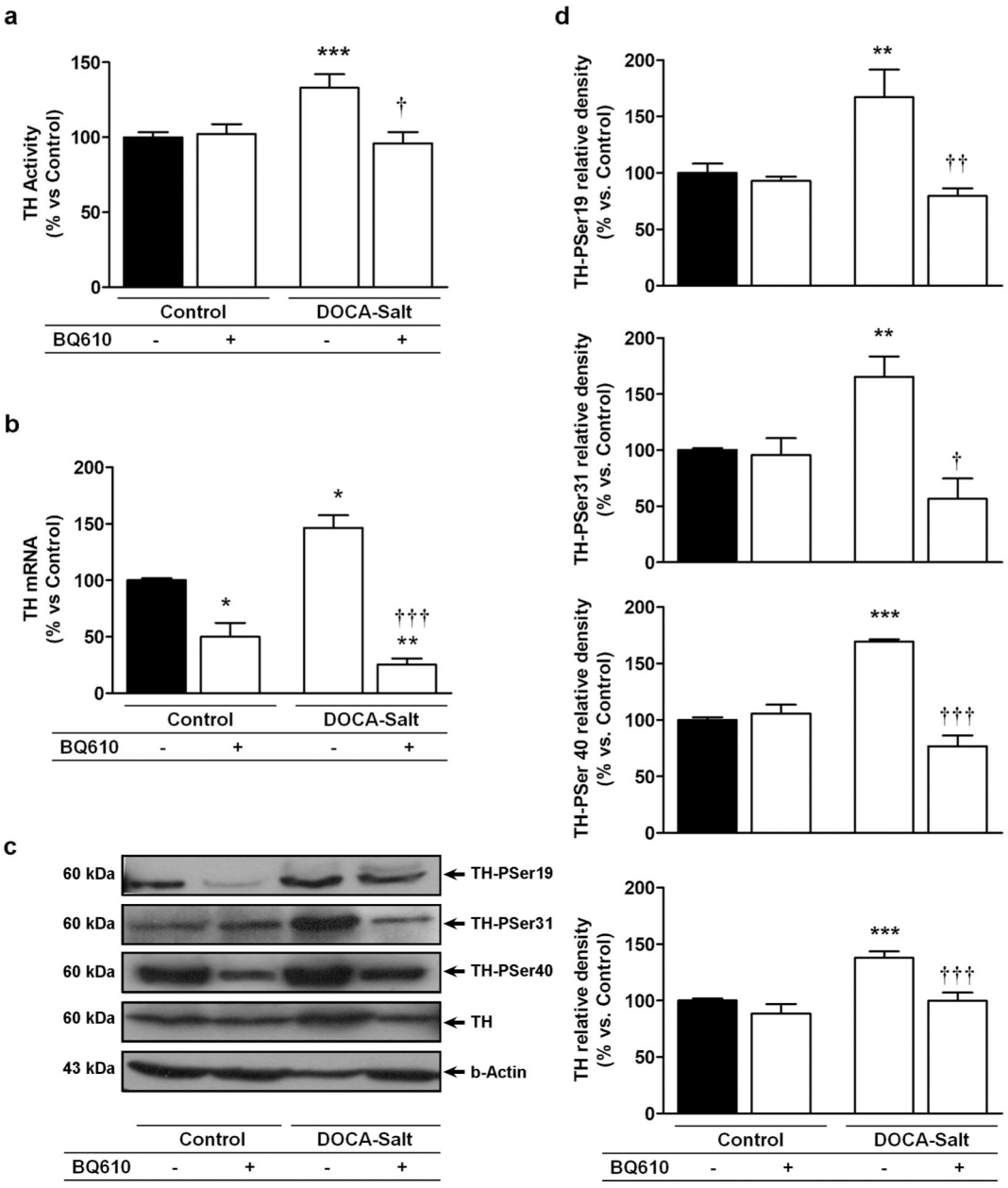

Figure 4: Tyrosine hydroxylase (TH) activity and expression in the olfactory bulb of normotensive and DOCA-Salt hypertensive rats following ET_A blockade.

TH **(a)** activity, **(d)** TH mRNA and **(b** and **c)** expression of total TH and its phosphorylated forms were assessed in the olfactory bulb at 60 min following artificial cerebrospinal fluid (Control) or BQ610 (selective ET_A antagonist) administration as detailed in Materials and Methods. *: $p<0.05$, **: $p<0.01$ and ***: $p<0.001$ *vs.* Control; †: $p<0.05$, ††: $p<0.01$, and †††: $p<0.001$ *vs.* DOCA-Salt. Number of animals per experimental group: 5-7.

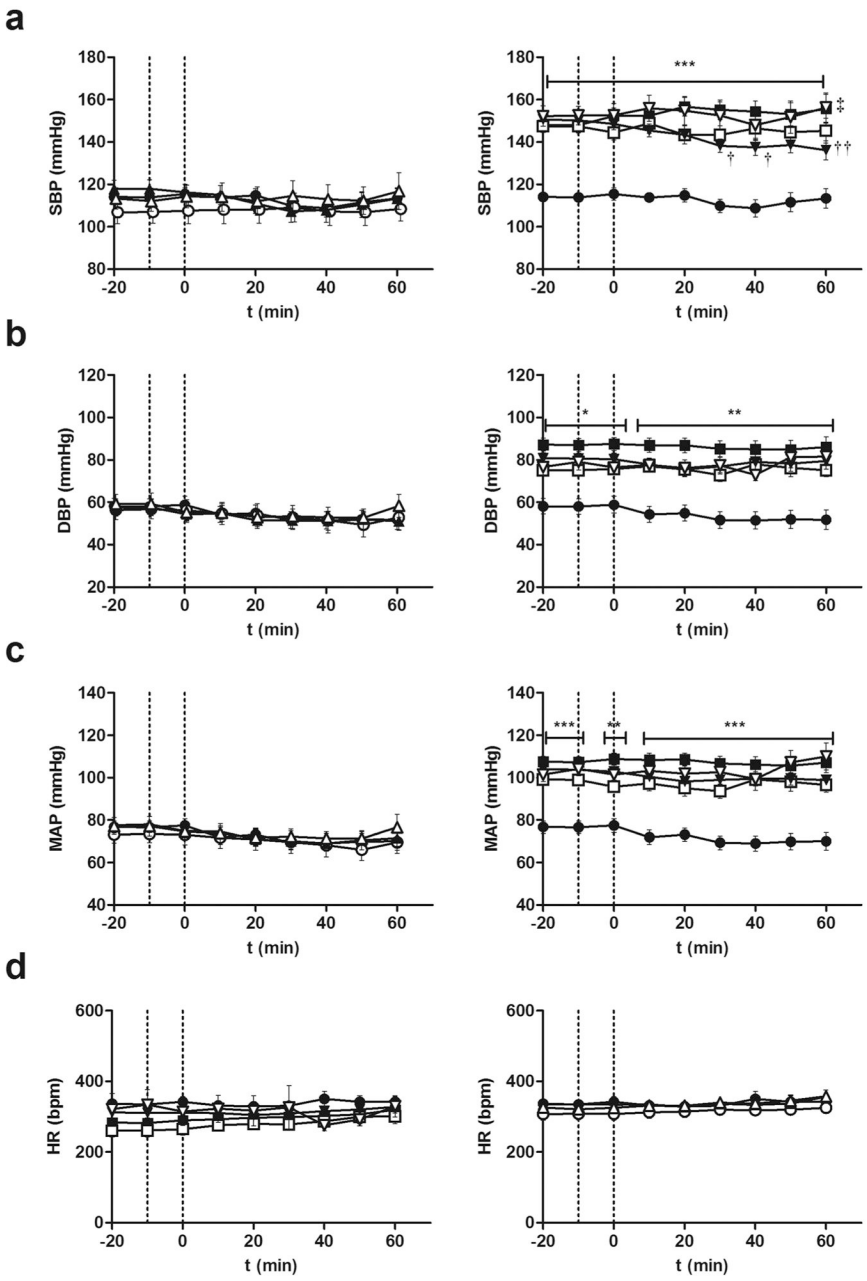

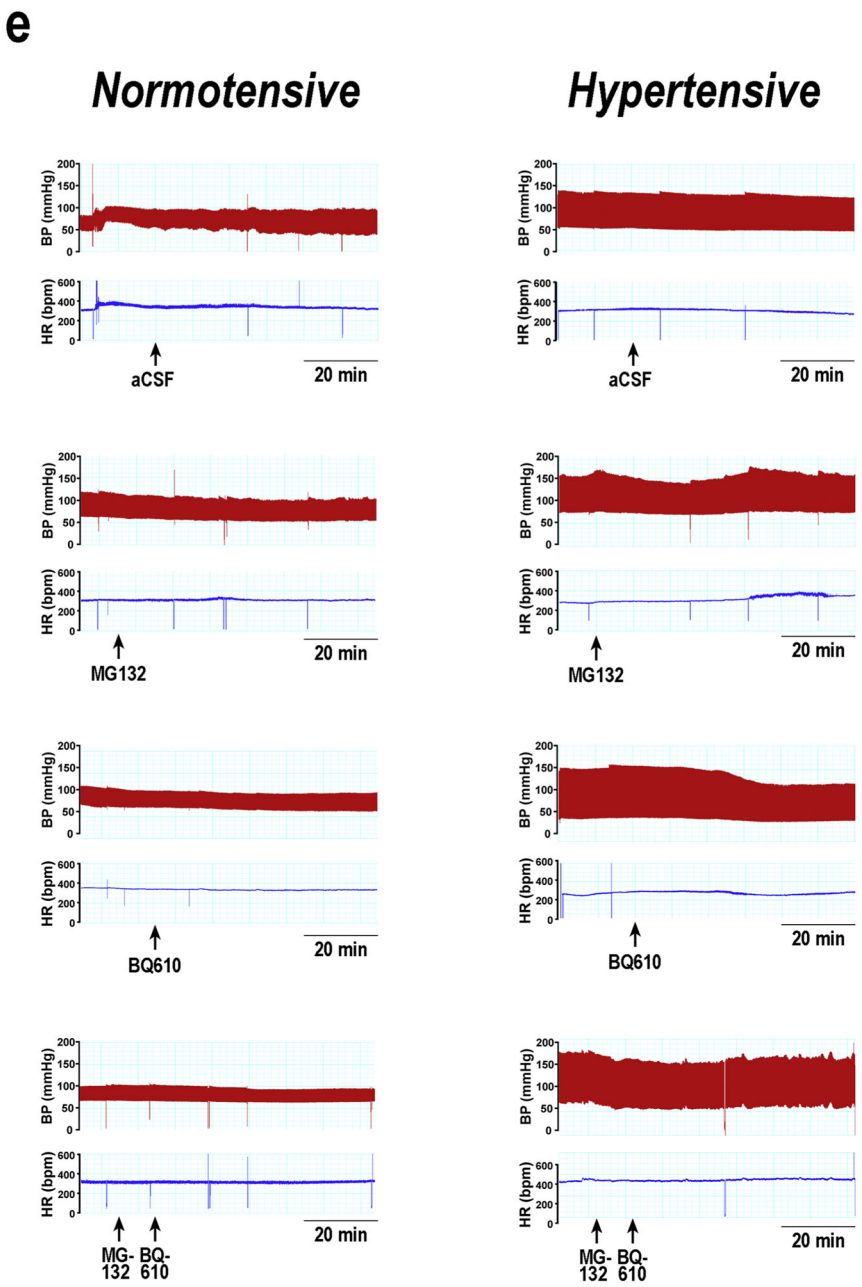

Figure 5: Hemodynamic parameters following proteasome inhibition and ET_A blockade in normotensive and DOCA-Salt hypertensive rats.

Time course (a) systolic blood pressure, (b) diastolic blood pressure, (c) mean arterial pressure (MAP) and (d) heart rate (HR) following MG132 (proteasome inhibitor) and BQ610 (selective ETA receptor antagonist) administration to normotensive (control) and hypertensive (DOCA-Salt) animals as detailed in Materials and Methods. (e) Representative traces of blood pressure and HR in normotensive and hypertensive rats following proteasome inhibition and ETA blockade. Control ●: +aCSF; ○: +MG132; ▲: +BQ610; Δ: +MG132+BQ610; DOCA-Salt ■: +aCSF; □: +MG132; ▼: +BQ610; ∇: +MG132+BQ610.

*: p<0.05, **p<0.01, ***p<0.001 *vs.* Control+aCSF; †: p<0.05, ††: p<0.01 *vs.* DOCA-Salt; ‡: p<0.05 *vs.* DOCA-Salt+BQ610. Number of animals per experimental group: 15-18.

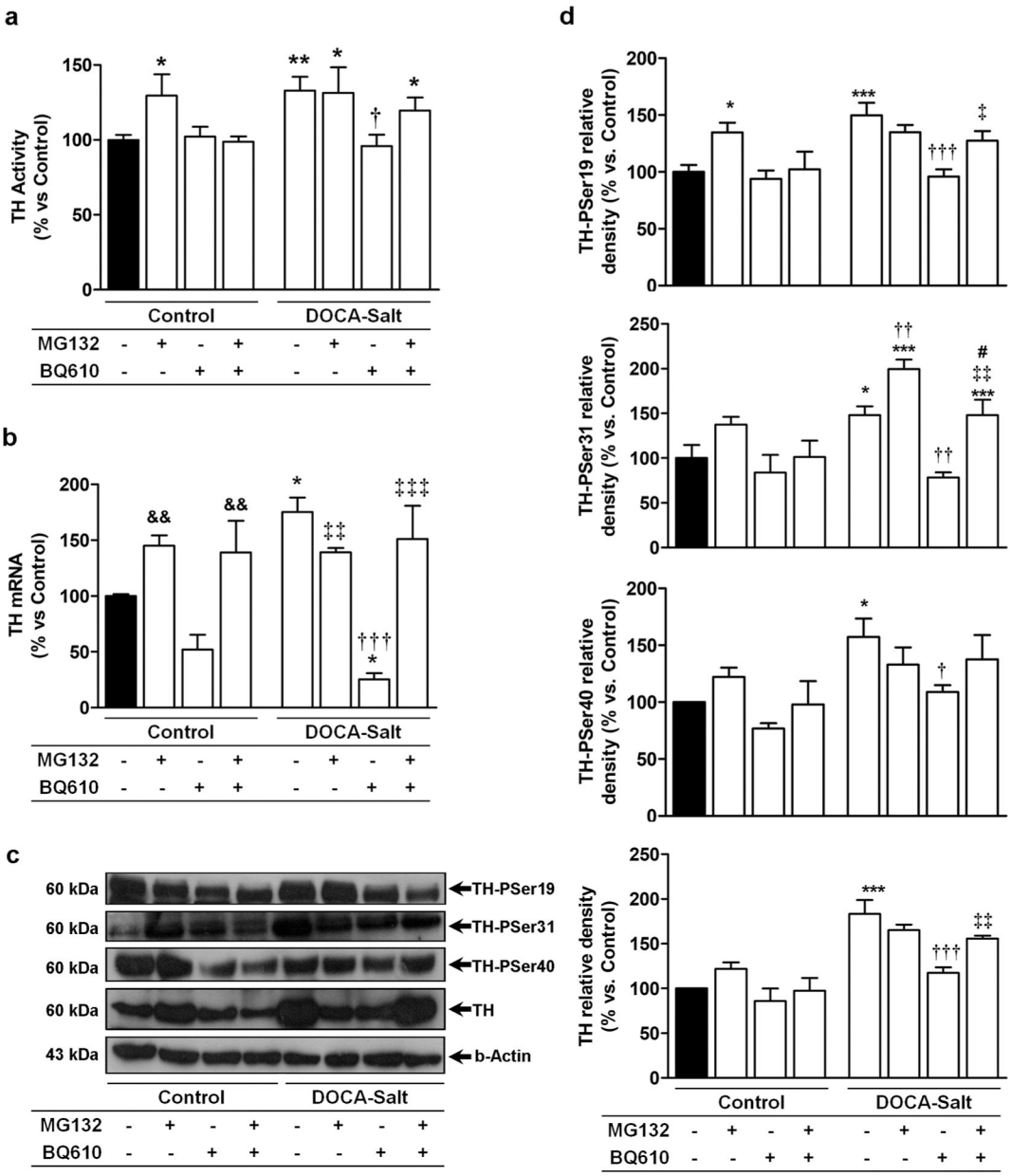

Figure 6: Tyrosine hydroxylase (TH) activity and expression in the olfactory bulb of normotensive and DOCA-salt hypertensive rats following proteasome inhibition and ET_A blockade.

(a) TH activity, **(b)** TH mRNA, **(c)** representative western blots and **(d)** densitometric analysis of total TH and its phosphorylated forms assessed in the OB following MG132 (proteasome inhibitor) (20 μM) and/or BQ610 (selective ET_A antagonist) (20 μM) administration as detailed in Materials and Methods. * p<0.05, ** p<0.01 and ***:p<0.001 vs Control; †: p<0.05, ††: p<0.01, and †††: p<0.001 vs. DOCA-Salt; ‡: p<0.05, ‡‡:p<0.01, and ‡‡‡: p<0.001 *vs.* DOCA-Salt+BQ610; &&: p<0.01 *vs.* BQ610; #: p<0.05 *vs.* DOCA-Salt+MG132. Number of animals per experimental group: 4-6.

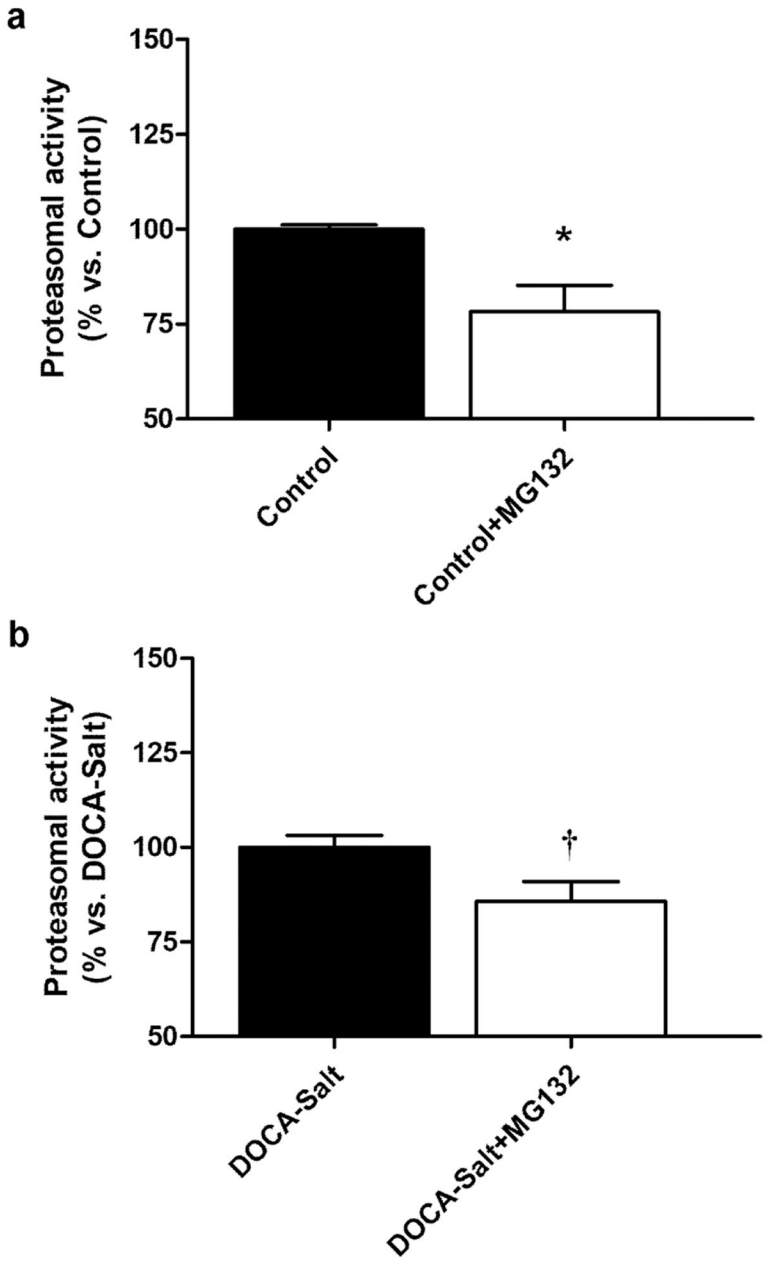

Figure 7: Proteasome activity.

Changes in proteasome activity following MG132 (20S proteasome inhibitor) administration to **(a)** normotensive rats and **(b)** DOCA-Salt hypertensive rats as detailed in Materials and Methods. *: $p<0.05$ vs Control; †: $p<0.05$ vs DOCA-Salt. Number of animals per experimental group: 4

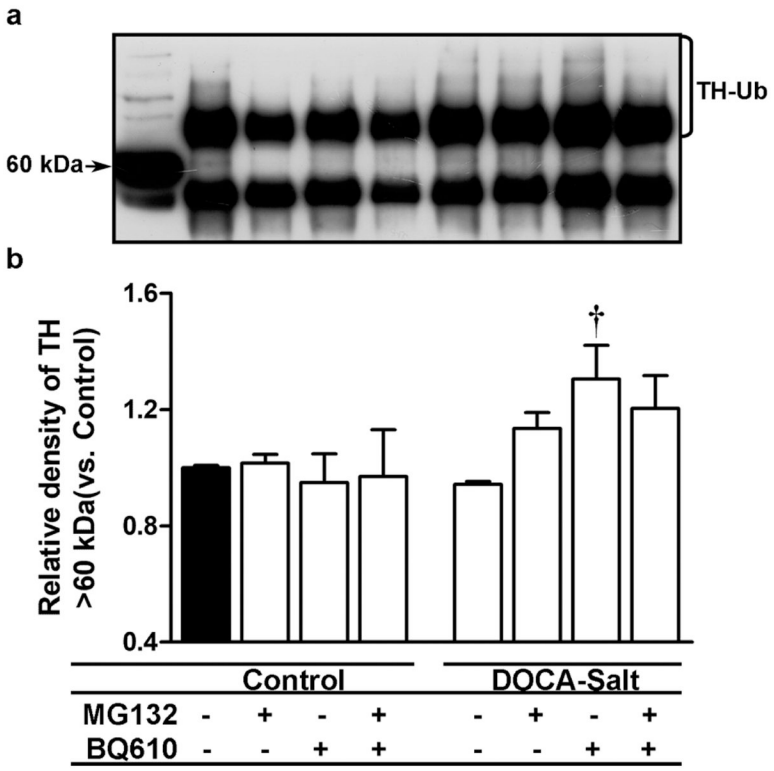

Figure 8: Ubiquitin-tagged tyrosine hydroxylase (TH) in the olfactory bulb of normotensive and DOCA-Salt hypertensive rats.

TH tagged with ubiquitin was assessed as detailed in Material and Methods in normotensive and DOCA-Salt hypertensive rats following the administration of MG132 (proteasome inhibitor) (20 μM), BQ610 (ET_A antagonist) (20 μM) alone or combined with MG132. **(a)** Representative immunoblot of ubiquitin-tagged TH. The first line shows a non-immunoprecipitated sample. **(b)** Densitometric analysis. †: $p<0.001$ *vs.* DOCA-Salt. Number of animals per experimental group: 4-5.

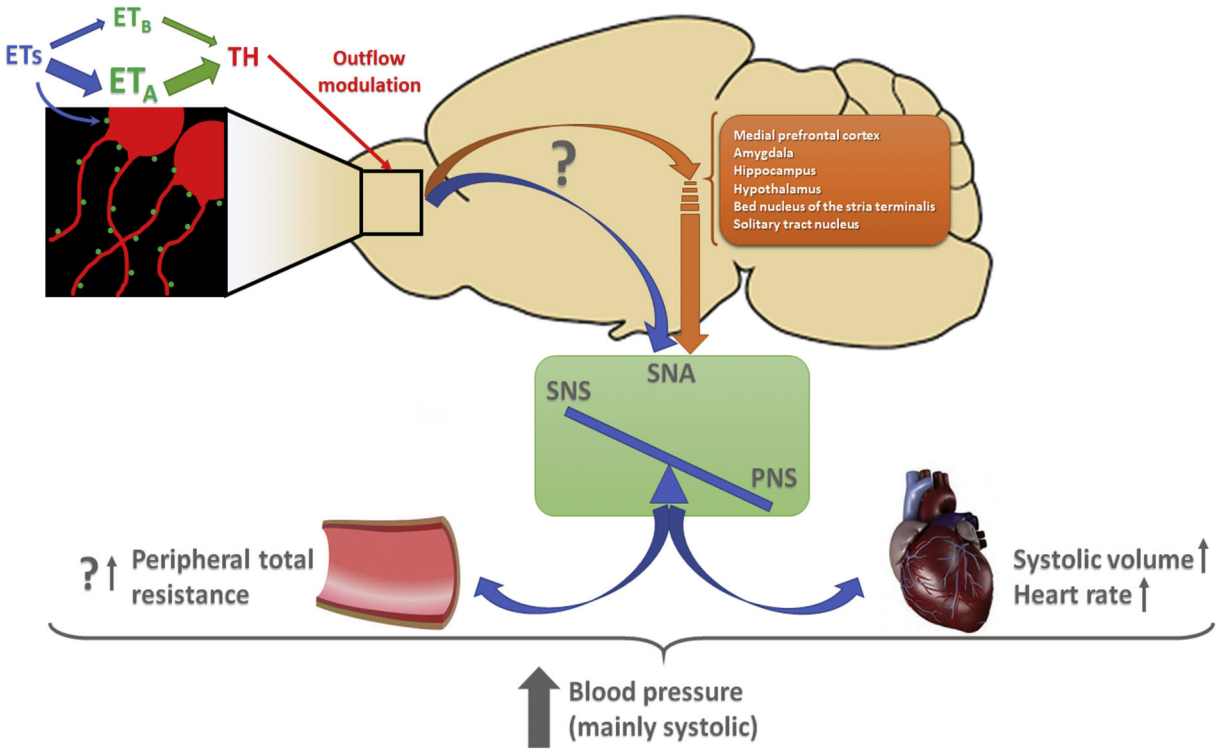

Figure 9: Proposed mechanism for catecholamine and ETs crosstalk in the OB and its contribution to chronic blood pressure elevation in DOCA-Salt hypertension.

In the glomerular lumen of the OB ET_A colocalizes with TH. In hypertensive rats increased ET_A expression would enhance TH activity and expression. Thus, the interneurons that affect the outflow of the projecting neurons (tuffed and mitral cells) would directly (blue arrow) and/or indirectly (orange arrow) modulate the information reaching the autonomic center resulting in sympathetic overflow, which would contribute to chronic blood pressure elevation. The relevance of this mechanism is revealed by acute ET_A blockade.

Table 1:
Antibodies Used in Fluorescence Microscopy.

Olfactory bulb slices were blocked with 10% normal horse serum for 1 h. Antibodies were diluted in phosphate buffered saline containing 0.3% Triton X-100 and 0.04% NaN_3. The entire procedure was conducted at room temperature.

Antibody	Manufacturer	Working solution	Incubation
Anti-ET_A	Alomone, Jerusalem, ISR	1:500	18-20 h in rocking agitation
Anti-TH	Sigma, Missouri, USA	1:10000	
Anti-Rabbit-Alexa488	Jackson, Pensilvania, USA	1:250	4 h in rocking agitation and light protected
Anti-Mouse-Alexa594	Jackson, Pensilvania, USA	1:250	
DAPI	Sigma, Missouri, USA	1:20000	Last 5 min of secondary antibody incubation
Anti-ET_A	Alomone, Jerusalem, ISR	1:500	18-20 h in rocking agitation
Anti-TH	Sigma, Missouri, USA	1:10000	
Anti-Rabbit-Alexa488	Jackson, Pensilvania, USA	1:250	4 h in rocking agitation and light protected
Anti-Mouse-Alexa594	Jackson, Pensilvania, USA	1:250	
DAPI	Sigma, Missouri, USA	1:20000	Last 5 min of secondary antibody incubation

Table 2:

Antibodies Used in Western Blot

All membranes were blocked with 5% non-fat milk in TBS-T for 1 h at room temperature. Antibodies were diluted in 1% non-fat milk in TBS-T.

Antibodies		Working solution	Incubation
Primary antibodies	Anti TH	1:2000	18-20 h at 4°C
	Anti β-Actin	1:2000	
	Anti TH-PSerl9	1:2000	
	Anti TH-PSer31	1:750	
	Anti TH-PSer40	1:2000	
	Anti ET-A	1:400	
	Anti ET-B	1:400	
Secondary antibodies	Anti-mouse (TH preincubation)	1:4000	90 min at room temperature with rocking agitation
	Anti-rabbit (β-actin preincubation)	1:4000	
	Anti-rabbit (TH-PSerl9 preincubation)	1:5000	
	Anti-rabbit (TH-PSer31 preincubation)	1:500	
	Anti-rabbit (TH-PSer40 preincubation)	1:5000	
	Anti-rabbit (ET-A preincubation)	1:2000	
	Anti-rabbit (ET-B preincubation)	1:2000	